

Requirement for *math5* in the development of retinal ganglion cells

Steven W. Wang,^{1,3} Byong Su Kim,^{1,3} Kan Ding,^{2,3} Huan Wang,² Dantong Sun,¹ Randy L. Johnson,¹ William H. Klein,¹ and Lin Gan^{1,2,4}

¹Department of Biochemistry and Molecular Biology, The University of Texas M. D. Anderson Cancer Center, Houston, Texas 77030, USA; ²Center for Aging and Developmental Biology, Box 645, University of Rochester, Rochester, New York 14642, USA

***math5* is a murine orthologue of *atonal*, a bHLH proneural gene essential for the formation of photoreceptors and chordotonal organs in *Drosophila*. The expression of *math5* coincides with the onset of retinal ganglion cell (RGC) differentiation. Targeted deletion of *math5* blocks the initial differentiation of 80% of RGCs and results in an increase in differentiated amacrine cells. Furthermore, the absence of *math5* abolishes the retinal expression of *brn-3b* and the formation of virtually all *brn-3b*-expressing RGCs. These results imply that *math5* is a proneural gene essential for RGC differentiation and that *math5* acts upstream to activate *brn-3b*-dependent differentiation processes in RGCs.**

Received September 27, 2000; revised version accepted November 20, 2000.

The mammalian retina is the peripheral portion of the visual system containing six major neuronal cell types and one glial cell type organized in a laminar structure. The visual information process in the retina follows a general pathway from photoreceptors to bipolar cells to retinal ganglion cells (RGCs). Horizontal cells and amacrine cells act to mediate lateral interactions among photoreceptors, bipolar cells, and RGCs. The latter serve as the sole output neurons in the retina to send the visual information down the optic nerve to the rest of brain. Both birthdating experiments using ³H-thymidine labeling and cell lineage analysis using retroviral and tracer-mediated approaches demonstrate that vertebrate retinal neurons are generated from common progenitors through sequential differentiation and ordered migration to form the laminar retinal structure (Cepko et al. 1996). Current models for retinal neuron differentiation suggest that the formation of a specific retinal neuron is deter-

mined by the intrinsic properties of the retinal progenitor and the extrinsic cues from the retinal environment (Cepko et al. 1996). Among the likely intrinsic factors, the basic helix-loop-helix (bHLH) class of proneural transcription factors appears to play an essential role in regulating the differentiation of retinal neurons (Cepko 1999). In *Drosophila*, expression of proneural genes of the *achaete-scute* complex (AS-C) and *atonal* (*ato*) in proneural clusters endow cells with neural competence (Jan and Jan 1993). Loss-of-function mutation of genes in AS-C causes the cells in the would-be proneural clusters to adopt epidermal fates rather than neuronal precursor fates. Conversely, gain-of-function mutations in the proneural genes leads to the ectopic formation of sensory neurons (Campuzano and Modolell 1992). The expression of *ato* is found in the optic furrow of the eye-antennal disc in addition to the ectodermal proneural clusters and sensory organ precursors, which give rise to the chordotonal organs. Deletion of *ato* causes the absence of the chordotonal organ and the lack of photoreceptors (Jarman et al. 1995), and the reduced expression of *ato* results in defects in axonal pathfinding of photoreceptors (White and Jarman 2000), suggesting that *ato* plays dual roles in determining neuronal potential and regulating specific neuronal differentiation events. Murine orthologs of many *Drosophila* proneural genes, including *NeuroD*, *mash1*, *math4a/Ngn2*, *math5*, and *math1*, are expressed in the developing retina and are thought to function as positive regulators of neuronal differentiation programs (Brown et al. 1998; Cepko 1999). Mutagenesis studies have shown that *mash1* regulates the formation of late-born retinal neurons, particularly the bipolar cells, and *NeuroD* acts to control the differentiation of amacrine and bipolar cells (Tomita et al. 1996; Morrow et al. 1999). While the differentiation of RGCs, the first-born retinal neurons, begins at embryonic day 11.5 (E11.5; Young 1985a), the retinal expression of *NeuroD*, *math1*, and *math4a/Ngn2* genes initiate at E13.5, and the retinal expression of *mash1* is not detected until E14.5 (Brown et al. 1998), indicating that none of the above bHLH genes is responsible for the initial differentiation of RGCs.

math5, an ortholog of *ato*, is transiently expressed in developing mouse retinas starting at E11, and its expression coincides with the differentiation of RGCs (Brown et al. 1998). Thus, *math5* is a good candidate for a proneural gene required for RGC formation. To investigate the role of *math5* in mouse retinal development and, particularly, in the development of RGCs, we used homologous recombination in murine embryonic stem (ES) cells to delete *math5*. We show here that targeted deletion of *math5* results in the loss of >80% of RGCs and of virtually all *brn-3b*-expressing RGCs and leads to an increase in differentiated amacrine cells. Expression properties of a reporter *lacZ* gene in *math5-lacZ* knock-in mice demonstrate that deletion of *math5* does not prevent the formation of RGC progenitors. However, *math5* deficiency leads to the loss of retinal expression of the

[Key Words: bHLH; *math5*; POU-domain; *brn-3b*; retinal development]

³These authors contributed equally to this article.

⁴Corresponding author.

E-MAIL lin_gan@urmc.rochester.edu; FAX (716) 756-7665.

Article and publication are at www.genesdev.org/cgi/doi/10.1101/gad.855301.

early RGC differentiation markers, *brn-3b* and *p75*, implying that the null mutation in *math5* blocks the initial differentiation of RGCs. The results imply that *math5* is essential for the initial differentiation of RGCs and that the loss of *math5* is likely to cause a cell-fate conversion of retinal progenitors from RGCs to amacrine cells. The effect of the *math5* mutation on the onset of *brn-3b* expression suggests that *math5* acts upstream to activate *brn-3b*-dependent differentiation processes in RGCs.

Results and Discussion

Targeted deletions of *math5* and retinal expression of a reporter *lacZ* gene

To investigate the role of *math5* in vivo, we generated a targeted deletion of *math5* by homologous recombination in ES cells. The mutant *math5* allele was created by replacing the entire *math5* open reading frame (ORF) with either a *lacZ* or *GFP* reporter gene (Fig. 1). Mice heterozygous for the *math5*-null allele appeared normal with no apparent retinal defects. Both heterozygous and homozygous *math5*-mutant mice were viable and fertile and had no discernible physical defects.

Previous in situ hybridization studies have shown that the retinal expression of *math5* was initiated at E11, before the onset of RGC differentiation. Its retinal expression was often observed in cells adjacent to proliferating regions (Brown et al. 1998). To determine whether the expression pattern of the knock-in *lacZ* gene faithfully reflected that of endogenous *math5* and to evaluate the possible effects of the *math5* mutation on retinal development, we compared *math5-lacZ* expression in the retinas of heterozygous and homologous mutant embryos. *math5-lacZ* expression in retinas of heterozygous embryos was first detected at E11 and peaked at E13.3, with

math5-lacZ-expressing cells distributed uniformly from the ventricular (proliferating) zone to the vitreous side (retinal ganglion layer) of the retina (Fig. 2A,C,E). After E13.5, *lacZ* expression was significantly reduced over the entire retina. At E15.5, robust expression was limited to the peripheral regions of the retina where RGCs were actively being generated, but much weaker expression was observed in more medial regions where RGCs were postmigratory (Fig. 2G). The *lacZ* expression in the ganglion cell layer (GCL) was likely to represent residual *lacZ* activity because endogenous *math5* expression is not found in differentiated RGCs (Brown et al. 1998). The overall expression pattern of *lacZ* in heterozygous embryonic retinas closely resembled that of endogenous *math5* (Brown et al. 1998) and indicated that the *math5* regulatory sequences in the *math5-lacZ* allele were sufficient to confer correct spatiotemporal expression. No notable differences in *lacZ* expression were seen when homozygous *math5-lacZ/math5-GFP* retinas from E11, E12.5, and E13.5 embryos were compared with similarly staged heterozygous *math5-lacZ/+* retinas (Fig. 2A–F), suggesting that a comparable number of *math5*-expressing cells were generated in heterozygous and homozygous *math5*-mutant retinas and that the expression of *math5* was not controlled by autoregulatory mechanisms as is the case for *ato* and *math1* (Jarman et al. 1995; Helms et al. 2000). However, in *math5-lacZ/math5-GFP* retinas at E15.5, we found a complete absence of the residual *lacZ* expression in GCL, which contrasted with the readily observable albeit weak expression in *math5-lacZ/+* retinas at the same stage (Fig. 2G,H). These results indicated that very few differentiated RGCs were forming in *math5*-deficient retinas.

Retinal ganglion cell defects of *math5*-null mice

To assess the potential loss of RGCs in *math5*-null retinas, we analyzed retinal sections prepared from postnatal mice at 3 wk of age, a time when all retinal neurons are fully developed (Young 1985b). The overall laminar structure of the homozygous *math5*-deficient retinas resembled those of wild-type and heterozygous retinas, and no noticeable changes in the number of photoreceptor cells in the outer nuclear layer (ONL) were observed. However, the mutant retinas were ~15%–20% thinner (Fig. 3A,B). This difference was mostly caused by the loss of >40% of the cells in GCL and the absence of a defined nerve fiber layer (NFL), which consists entirely of bundles of RGC axons (Fig. 3A,B). In mice, RGCs and displaced amacrine cells each constitute about one-half of the cells in GCL (Perry 1981; Barnstable and Drager 1984). Therefore, the 40% or more loss of cells in GCL could account for a >80% loss of RGCs. Quantification of the number of axon bundles in retinas immunostained with SMI-32, a mouse monoclonal antibody that reacts with neurofilament H and labels predominantly the axons of large ganglion cells

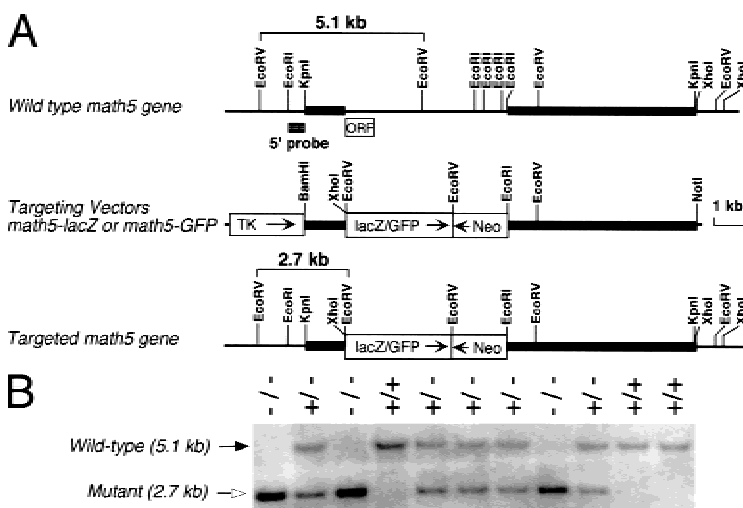


Figure 1. Targeted deletion and expression of *math5*. (A) *math5* genomic structure, restriction enzyme map, and targeting strategy. The DNA fragment containing the *math5* ORF region was replaced with *GFP* or *lacZ* in the targeting vector. Neo, PGK-neo cassette; TK, MCI-TK cassette. (B) Southern genotyping of a typical litter from a heterozygous cross. The 5' probe detected 5.1-kb wild-type and 2.7-kb mutant *EcoRV* fragments.

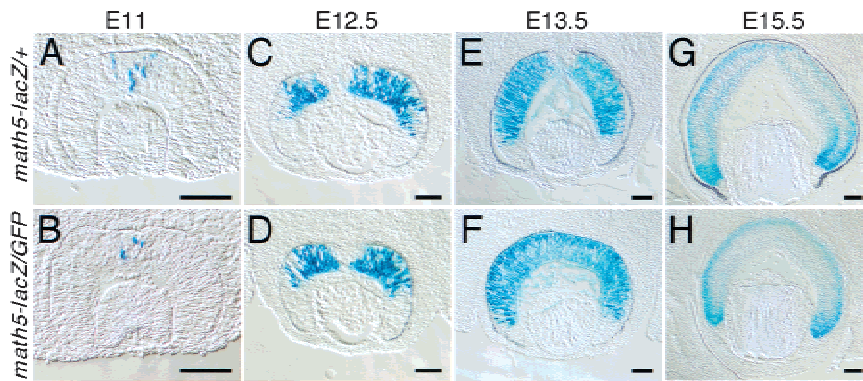


Figure 2. Expression of the *math5-lacZ* fusion gene in developing retinas. The *math5* heterozygous (*math5-lacZ/+*) and homozygous (*math5-lacZ/GFP*) retinas were collected for whole-mount staining of *lacZ* activities. After staining, the retinas were cryosectioned and photographed using DIC-Nomarski optics. The *math5-lacZ* expression was first detected in the central region of developing retina at E11.5 (A,B). At E12.5 (C,D) and E13.5 (E,F), *math5-lacZ* expression rapidly expanded throughout the retinas. After peaking at E13.5, high-level expression was limited to the peripheral regions of the retina (G,H), where RGCs are being generated. Scale bar, 100 μ m.

(Nixon et al. 1989), showed an ~80% reduction of SMI-32-positive processes in *math5*-null retinas (118 ± 12 axon bundles) relative to wild-type controls (583 ± 24.8 axon bundles; Fig. 3C,D). The remaining 20% of the SMI-32-positive processes appeared to form axon bundles, projected toward the optic disk region, and formed a very thin optic nerve and optic chiasm (Fig. 3D; data not shown). However, many of these axon bundles were abnormally curved, suggesting a defect in axon pathfinding during development.

In previous studies, we showed that the Class IV *POU* domain-containing *brn-3b* gene was required for the terminal differentiation of RGCs and that null mutations in *brn-3b* resulted in axon growth defects and programmed cell death in ~70% of newly formed RGCs (Gan et al. 1996, 1999). The loss of RGCs observed in the *math5*-deficient mice resembled that of *brn-3b*-null mice. To test whether *math5* and *brn-3b* were involved in the differentiation of the same population of RGCs, we generated mice with compound mutations in *math5* (*math5-GFP*) and *brn-3b* (*brn-3b-lacZ*). Nuclear expression of *lacZ* in *brn-3b-lacZ* mice serves to effectively mark *brn-3b*-positive RGCs (Gan et al. 1999). Compared with normal retinas (*brn-3b-lacZ/+*, *math5+/+*), *math5*-null retinas (*brn-3b-lacZ/+*, *math5-GFP/math5-GFP*) showed a loss of ~97% of *brn-3b-lacZ*-expressing cells (1678 ± 26 cells/mm² express *brn-3b-lacZ* in normal retinas, as compared with 47 ± 2.6 cells/mm² in *math5*-null retinas; Fig. 3E,F), thus demonstrating that *math5* was required for the differentiation of most *brn-3b*-expressing RGCs. The remaining RGCs in *math5*-deficient retina appeared to be expressing *brn-3b* but were generated by a *math5*-independent pathway.

Absence of early RGC differentiation in *math5*-null retinas

The absence of 80% of RGCs in mature *math5*-deficient retinas could be the result of an insufficient number of

RGC progenitors or a failure of RGC differentiation or survival. Because a similar number of *math5-lacZ*-expressing cells were detected in heterozygous and homozygous *math5*-mutant retinas between E11 and E15.5 (Fig. 2), it was unlikely that there were an insufficient number of progenitor cells. TUNEL analysis also revealed no overt difference in apoptosis in retinas at E12.5–E19 in *math5*-deficient and wild-type embryos (data not shown). A reasonable hypothesis was that *math5*-deficient retinas were unable to form RGCs. To test whether *math5*-null retinal progenitor cells failed to differentiate into RGCs, we examined the presence of newly differentiated RGCs by detecting the expression of the early RGC markers, *brn-3b* and *p75*, the latter of which encodes a receptor for nerve growth factor (NGF) and neurotrophins (Frade and Barde 1999; Gan et al. 1999). Section in situ hybridization with a *brn-3b* antisense probe and expression of the *brn-3b-lacZ* allele at E13.5 showed that *brn-3b* was highly expressed in wild-type retinas (Fig. 4C,E) but was virtually absent in homozygous *math5*-null retinas (Fig. 4D,F). Similarly, immunostaining of E13.5 retinas with anti-p75 showed that the expression of *p75* in *math5*-deficient retina was severely reduced (Fig. 4G,H). The absence of most RGCs in mature *math5*-deficient retinas, and the lack of *brn-3b* and *p75* expression in *math5*-deficient embryonic retinas, argued strongly that in *math5*-null retinas, retinal progenitor cells were unable to differentiate into RGCs. Because *brn-3b* expression was essentially absent in *math5*-null retinas, the results also demonstrated that *math5* was genetically upstream of *brn-3b*.

Effects of *math5* mutation on other retinal neurons

In *Drosophila*, *ato* is required for the specification of the founder photoreceptors—the R8 cells, which in turn recruit the other photoreceptors (Jarman et al. 1995). Current models of retinal neuron differentiation suggest that the cell differentiation of RGCs is negatively regulated through a feedback mechanism by the presence of differentiated RGCs (Cepko et al. 1996; Belliveau and Cepko 1999; Belliveau et al. 2000). However, it remains unclear how the loss of RGCs could influence the formation of other retinal neurons. In addition, the lack of appropriate synaptic connections in the absence of most RGCs is likely to have pronounced effects on neurons in the inner nuclear layer (INL). To determine whether the *math5* mutation affected the development of retinal neurons other than RGCs, we monitored the expression of Protein Kinase C- α (PKC- α) as a bipolar cell marker (Wassle and Boycott 1991) and syntaxin and choline acetyltransferase (ChAT) as amacrine cell markers (Barnstable et al. 1985; Jeon et al. 1998) in mature retina.

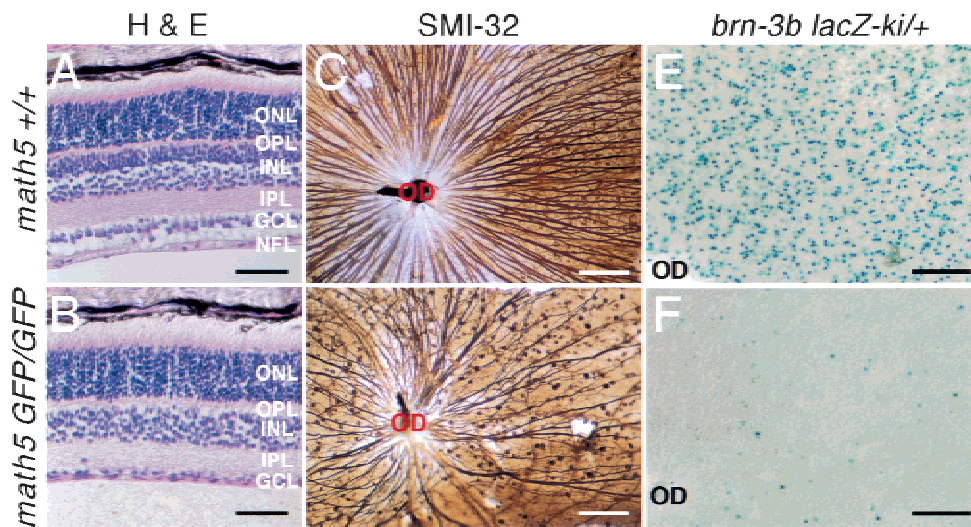


Figure 3. Reduction in the number of retinal ganglion cells in *math5*-mutant retinas. Retinas from 3-wk-old *math5* wild-type (*math5*^{+/+}) and mutant (*math5* *GFP/GFP*) mice were analyzed by haematoxylin and eosin (H&E) staining (A,B), whole-mount immunostaining with SMI-32 (C,D), and X-Gal staining for *brn-3b-lacZ* expression (E,F). Retinal neurons are organized in a layered structure with photoreceptors (cones and rods) located in the outer nuclear layer (ONL), interneurons (bipolar, horizontal, and amacrine cells) in the inner nuclear layer (INL), and retinal ganglion cells (RGCs) and displaced amacrine cells in the ganglion cell layer (GCL). The synaptic contacts among retinal neurons are restricted to two defined layers. The outer plexiform layer (OPL) contains the synaptic contacts among photoreceptor, bipolar, and horizontal cells, and the inner plexiform layer (IPL) consists of the synaptic connections among bipolar, amacrine, and ganglion cells. Ganglion nerve fiber layer (NFL) consists of axons of RGCs. In *math5*-mutant retinas, the thickness of the ONL remains unchanged. However, the number of cells in the GCL dropped significantly, and the thickness of NFL was greatly reduced (B). SMI-32 and *lacZ* expression revealed the loss of >80% of total RGCs and most of the *brn-3b*-expressing RGCs in mutant retinas (C–F). OD, optic disc. Scale bar, 50 μ m in A and B, 100 μ m in C and D, and 200 μ m in E and F.

PKC- α is expressed in cell bodies and processes of bipolar cells that mainly connect to rods (Wassle and Boycott 1991). In wild-type retinas, PKC- α labeled cells in

the inner nuclear layer and axons and dendrites within the outer and inner plexiform layer (Fig. 5A). In *math5*-mutant retina, the labeling pattern and the number of

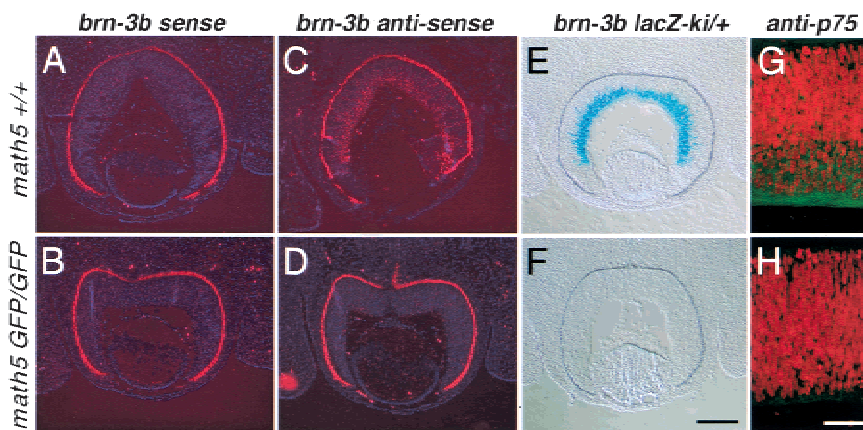


Figure 4. Absence of newborn RGCs in *math5*-null retinas at E13.5. Retinal sections from wild-type (A,C) and *math5*-null (B,D) mice were probed with *brn-3b* sense (A,B) and antisense (C,D) probes in sectioned in situ hybridization. *brn-3b* was expressed at high levels in the RGC layer in wild-type retina (C), but its expression was severely reduced in *math5*-null retina (D). *brn-3b* sense probe served as an in situ hybridization control. Similarly, the expression of *brn-3b-lacZ* was in heterozygous *brn-3b lacZ* retinas in a *math5* wild-type background (E) but not in *math5*-null background (F). Immunostaining with anti-p75 (green) revealed the accumulation of p75 in newly formed RGCs in wild-type retina at E13.5 (G) but not in *math5*-deficient retina (H). Nuclei in G and H were counterstained with propidium iodide (red). Scale bar, 200 μ m in A–F and 50 μ m in G and H.

PKC- α -expressing cells were similar to those in the wild-type retinas, indicating that *math5*-null mutation had no apparent effects on the bipolar cells expressing PKC- α .

In contrast to bipolar cells, amacrine cells were noticeably affected by the loss of *math5*. Expression of both syntaxin and ChAT were strongly upregulated when compared to wild-type controls (Fig. 5C–F). Quantitation of the number of ChAT-positive cells demonstrated a 7.5-fold increase in *math5*-null retinas (93 ± 12 ChAT-expressing cells/0.04 mm²) relative to wild-type controls (12.3 ± 3.3 ChAT-expressing cells/0.04 mm²). Moreover, most of the syntaxin- and ChAT-positive cells were located in GCL rather than the inner nuclear layer. In vertebrates, starburst amacrine cells are the only cholinergic retinal cells, and the cholinergic amacrine cells in GCL are the ON-starburst amacrine cells. Our data suggested that the loss

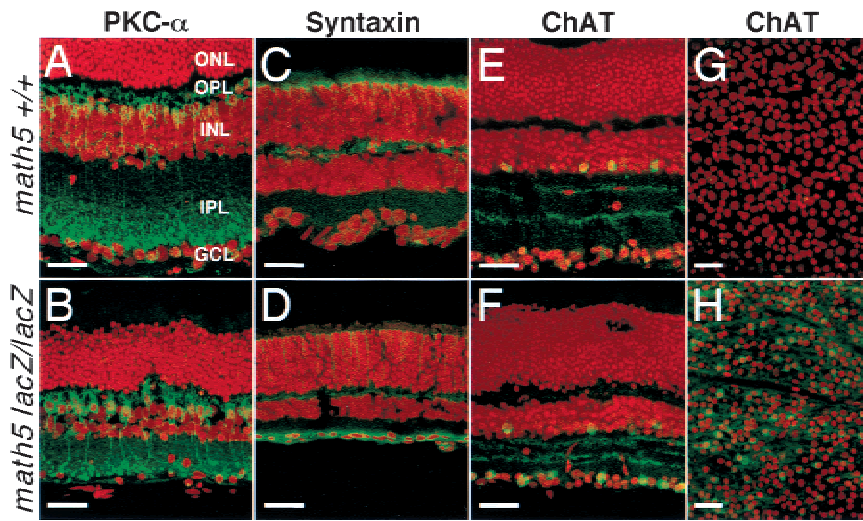


Figure 5. Effect of the *math5*-null mutation on bipolar and amacrine cells in adult retinas. Retinas were immunolabeled with antibodies (green) and counter-stained for nuclei with propidium iodide (red). No significant changes were detected in *math5*-null retina in the number of bipolar cells as shown by anti-PKC- α expression (A,B). Antisyntaxin (C,D) and anti-ChAT (E,F, and in whole-mount, G,H) labeling demonstrated an increased number of amacrine cells in *math5*-null retinas, in particular a 7.5-fold increase in the number of cholinergic amacrine cells labeled by anti-ChAT. Scale bar, 30 μ m.

of *math5* resulted in an increase of amacrine cells, in particular the ON-starburst amacrine cells, and their displacement to GCL. Most likely, the displacement of amacrine cells was caused by the loss of retinal ganglion cells. Based on cell birthdating experiments, amacrine cells are among the early-born neurons in the mouse retina and are generated at approximately the same time as RGCs (Cepko et al. 1996). Thus, it is possible that in *math5*-null retinas, progenitor cells unable to form RGCs switch their fate to the amacrine cell differentiation pathway. It is also possible that *math5* is expressed in amacrine cell lineages during normal retinal development and negatively controls the differentiation of amacrine cells. However, if *math5* acts like the other *atonal*-class bHLH proneural genes to promote the differentiation of specific neurons, it is most likely that *math5* is expressed only in RGC lineages and promotes their differentiation rather than in amacrine cell lineages to inhibit their differentiation.

Given that the majority of RGCs did not differentiate at early stages of retinal development, the fact that the resulting retina maintained its structural integrity and contained all other neuronal cell types was unexpected. Our results indicated that the developmental relationships among the retinal cell types are not tightly regulated and that the lack of majority of RGCs does not dramatically affect the overall patterning of the retina.

Several investigations have shown that the *Notch-Delta* pathway is important for negatively regulating the differentiation of RGCs and other neurons in the retina (Austin et al. 1995; Dorsky et al. 1995; Bao and Cepko 1997). The *Notch-Delta* pathway likely acts to negatively regulate the expression of proneural genes like

math5 in the mouse retina, as is the case for *ato* in the *Drosophila* eye. Because *math5* encodes a bHLH transcriptional factor, it must function by regulating genes required for RGC differentiation. In *Drosophila*, *ato* functions to regulate the formation and axon pathfinding properties of R8 photoreceptors (White and Jarman 2000). However, the molecular mechanisms of its function in axon pathfinding and other neural terminal differentiation processes remain poorly understood. Our studies showed that *math5*- and *brn-3b*-null mutations affect the development of largely the same population of RGCs and that *math5* appears to be genetically upstream of *brn-3b*. Combined with our early studies that *brn-3b* is involved in normal axon growth of mouse RGCs (Gan et al. 1999; Wang et al. 2000), our results indicate that although the morphological and physiological properties of R8 photoreceptors in *Drosophila* and RGCs in mice are highly diverged, a conserved

genetic regulatory pathway may control the differentiation of both of these cell types. The down-regulation of the *Notch-Delta* signaling pathway leads to the up-regulation of *ato/math5*, which in turn activates downstream effector genes like *brn-3b* to promote R8/RGC differentiation and normal axonal outgrowth. It remains to be determined whether *math5* activates *brn-3b* directly during normal retinal development. The results presented here demonstrate that the proneural gene *math5* is essential for the differentiation of RGCs and that a null mutation of *math5* results in the failure of the majority of RGCs to form.

Previous studies have shown that targeted expression of *Xath5*, a *math5* ortholog in *Xenopus*, in the optic vesicle promotes the generation of RGCs, suggesting that *Xath5* is sufficient to direct the differentiation of retinal progenitors into RGCs (Kanekar et al. 1997). Whether or not *math5* is sufficient for RGC in the mouse can be tested by ectopic expression of *math5* in retinal progenitors. In addition, while *ato* is required for the generation of all R8 cells, *math5* was essential for the appearance of the majority of RGCs. It is likely that in mouse, other genes, particularly other proneural bHLH genes expressed in the retina, could account for the remaining RGCs.

Materials and methods

Targeted deletion of *math5*

Mouse *math5* genomic sequences were isolated from a mouse genetic DNA library (Strain 129/SvEv) in λ DASHII (Stratagene), using *math5* cDNA (L. Gan, unpubl.) as a probe. Targeted mutation of *math5* was generated by inserting the *math5* 1.5-kb 5' sequences containing the entire 5' untranslated region and the 5.8-kb 3' sequences into the *Bam*HI/*Xho*I and *Eco*RI/*Not*I sites in the 5' and 3' multiple cloning sites

of pKI-*lacZ* or pKI-*GFP* vectors (L. Gan, unpubl.), respectively. The constructs place the *lacZ* and *GFP* under the control of *math5* regulatory sequences. Generation of mutant mice, genotyping, and X-Gal staining were done as described (Gan et al. 1996, 1999). All analysis was done on a mixed C57B6/J and 129/SvEv background. To compare the number of *brn-3b-lacZ*-expressing cells, three *math5* wild-type and three *math5* mutant retinas from two litters at 3 wk old were whole-mount stained for *lacZ* activities, and the number of *brn-3b-lacZ* positive cells were counted in an 800 × 1200 μm field adjacent to the optic disc.

Sectioned in situ hybridization

Sectioned in situ hybridization was conducted as described (Riddle et al. 1993). To generate *brn-3b* probes, the mouse 3.1-kb *brn-3b* cDNA clone was isolated from a mouse E14.5 retina cDNA library (L. Gan, unpubl.) in pBluescript SKII(+) (Stratagene). The cDNA clone was linearized with *XhoI* and *XbaI* for synthesis of sense and antisense probes using T3 and T7 RNA polymerase, respectively.

Immunohistochemistry and microscopy

Immunohistochemical staining of whole-mount retinas using SMI-32 (Sternberger Monoclonals) was done as described (Gan et al. 1996). Counts of SMI-32-expressing RGCs were compared in four wild-type and three *math5* mutant retinas from mice at 3 wk old. To quantify the number of SMI-32-positive RGCs, micrographs of the whole-mount stained retinas were taken and the total numbers of axon bundles were counted at the circumference ~500 μm from the optic disc.

For confocal microscopy, retinal tissues from different ages were fixed with 3.2% paraformaldehyde in PBS (pH 7.4) for 30 min at room temperature. Fixed samples were washed three times with PBS and cryosectioned to a thickness range from 15 to 25 μm. Sections were incubated 30 min in PBS containing 0.05% Triton X-100 (PBS-T) and blocked with 2% BSA in PBS-T for 1 h. Sections were then incubated sequentially for 1 h, each with the primary antibody and secondary antibody. Sections were washed three times with PBS-T between the antibody incubations. Primary antibodies used were mouse anti-rat syntaxin (Sigma, S0664), rabbit antihuman choline acetyltransferase (Chemicon, AB143), rabbit antimouse PKC-α (Sigma, P4334), and rabbit antihuman p75 (Promega, G323A). Secondary antibodies used were Alexa 488-conjugated anti-mouse or anti-rabbit IgG (Molecular Probes). Antibody-labeled sections were treated with 0.05% propidium iodide for 2 min at room temperature. Prepared sections were mounted in Fluoromount (EMS) and examined using a Zeiss 410 or a Olympus FV300 confocal microscope. Images were projected from eight optical sections with intervals of 0.5 μm. Projected images were pseudocolored to restore the colors as seen in an epifluorescent microscope. To quantify the number of ChAT-positive amacrine cells, three wild-type and three *math5*-mutant retinas from the same litter were whole-mount stained with anti-ChAT antibody, and the counts were done on micrographs in a 200 × 200 μm field.

Acknowledgments

We thank Q. Fu and M. Wu for technical assistance and Jose Luis de la Pompa for critical reading of the manuscript. This work was supported by the Silbermann Foundation and Retinal Research Foundation (L.G.) and an NEI grant RO1EY11930 and the Welch Foundation (W.H.K.).

The publication costs of this article were defrayed in part by payment of page charges. This article must therefore be hereby marked "advertisement" in accordance with 18 USC section 1734 solely to indicate this fact.

References

Austin, C.P., Feldman, D.E., Ida, Jr., J.A., and Cepko, C.L. 1995. Vertebrate retinal ganglion cells are selected from competent progenitors by the action of Notch. *Development* **121**: 3637–3650.
 Bao, Z.Z. and Cepko, C.L. 1997. The expression and function of Notch pathway genes in the developing rat eye. *J. Neurosci.* **17**: 1425–1434.
 Barnstable, C.J. and Drager, U.C. 1984. Thy-1 antigen: A ganglion cell specific marker in rodent retina. *Neuroscience* **11**: 847–855.
 Barnstable, C.J., Hofstein, R., and Akagawa, K. 1985. A marker of early amacrine cell development in rat retina. *Brain Res.* **352**: 286–290.
 Belliveau, M.J. and Cepko, C.L. 1999. Extrinsic and intrinsic factors con-

trol the genesis of amacrine and cone cells in the rat retina. *Development* **126**: 555–566.
 Belliveau, M.J., Young, T.L., and Cepko, C.L. 2000. Late retinal progenitor cells show intrinsic limitations in the production of cell types and the kinetics of opsin synthesis. *J. Neurosci.* **20**: 2247–2254.
 Brown, N.L., Kanekar, S., Vetter, M.L., Tucker, P.K., Gemza, D.L., and Glaser, T. 1998. Math5 encodes a murine basic helix–loop–helix transcription factor expressed during early stages of retinal neurogenesis. *Development* **125**: 4821–4833.
 Campuzano, S. and Modolell, J. 1992. Patterning of the *Drosophila* nervous system: The achaete-scute gene complex. *Trends Genet.* **8**: 202–208.
 Cepko, C.L. 1999. The roles of intrinsic and extrinsic cues and bHLH genes in the determination of retinal cell fates. *Curr. Opin. Neurobiol.* **9**: 37–46.
 Cepko, C.L., Austin, C.P., Yang, X., Alexiades, M., and Ezzeddine, D. 1996. Cell fate determination in the vertebrate retina. *Proc. Natl. Acad. Sci.* **93**: 589–595.
 Dorsky, R.L., Rapaport, D.H., and Harris, W.A. 1995. Xotch inhibits cell differentiation in the *Xenopus* retina. *Neuron* **14**: 487–496.
 Frade, J.M. and Barde, Y.A. 1999. Genetic evidence for cell death mediated by nerve growth factor and the neurotrophin receptor p75 in the developing mouse retina and spinal cord. *Development* **126**: 683–690.
 Gan, L., Xiang, M., Zhou, L., Wagner, D.S., Klein, W.H., and Nathans, J. 1996. POU domain factor Brn-3b is required for the development of a large set of retinal ganglion cells. *Proc. Natl. Acad. Sci.* **93**: 3920–3925.
 Gan, L., Wang, S.W., Huang, Z., and Klein, W.H. 1999. POU domain factor Brn-3b is essential for retinal ganglion cell differentiation and survival but not for initial cell fate specification. *Dev. Biol.* **210**: 469–480.
 Helms, A.W., Abney, A.L., Ben-Arie, N., Zoghbi, H.Y., and Johnson, J.E. 2000. Autoregulation and multiple enhancers control Math1 expression in the developing nervous system. *Development* **127**: 1185–1196.
 Jan, Y.N. and Jan, L.Y. 1993. HLH proteins, fly neurogenesis, and vertebrate myogenesis. *Cell* **75**: 827–830.
 Jarman, A.P., Sun, Y., Jan, L.Y., and Jan, Y.N. 1995. Role of the proneural gene, *atonal*, in formation of *Drosophila* chordotonal organs and photoreceptors. *Development* **121**: 2019–2030.
 Jeon, C.J., Strettoi, E., and Masland, R.H. 1998. The major cell populations of the mouse retina. *J. Neurosci.* **18**: 8936–8946.
 Kanekar, S., Perron, M., Dorsky, R., Harris, W.A., Jan, L.Y., Jan, Y.N., and Vetter, M.L. 1997. Xath5 participates in a network of bHLH genes in the developing *Xenopus* retina. *Neuron* **19**: 981–994.
 Morrow, E.M., Furukawa, T., Lee, J.E., and Cepko, C.L. 1999. NeuroD regulates multiple functions in the developing neural retina in rodent. *Development* **126**: 23–36.
 Nixon, R.A., Lewis, S.E., Dahl, D., Marotta, C.A., and Drager, U.C. 1989. Early posttranslational modifications of the three neurofilament subunits in mouse retinal ganglion cells: Neuronal sites and time course in relation to subunit polymerization and axonal transport. *Brain Res. Mol. Brain Res.* **5**: 93–108.
 Perry, V.H. 1981. Evidence for an amacrine cell system in the ganglion cell layer of the rat retina. *Neuroscience* **6**: 931–944.
 Riddle, R.D., Johnson, R.L., Laufer, E., and Tabin, C. 1993. Sonic hedgehog mediates the polarizing activity of the ZPA. *Cell* **75**: 1401–1416.
 Tomita, K., Nakanishi, S., Guillemot, F., and Kageyama, R. 1996. Mash1 promotes neuronal differentiation in the retina. *Genes Cells* **1**: 765–774.
 Wang, S.W., Gan, L., Martin, S.E., and Klein, W.H. 2000. Abnormal polarization and axon outgrowth in retinal ganglion cells lacking the POU-domain transcription factor Brn-3b. *Mol. Cell. Neurosci.* **16**: 141–156.
 Wassle, H. and Boycott, B.B. 1991. Functional architecture of the mammalian retina. *Physiol. Rev.* **71**: 447–480.
 White, N.M. and Jarman, A.P. 2000. *Drosophila* *atonal* controls photoreceptor R8-specific properties and modulates both receptor tyrosine kinase and Hedgehog signalling. *Development* **127**: 1681–1689.
 Young, R.W. 1985a. Cell differentiation in the retina of the mouse. *Anat. Rec.* **212**: 199–205.
 ———. 1985b. Cell proliferation during postnatal development of the retina in the mouse. *Brain Res.* **353**: 229–239.